New enhancement of infrared image based on human visual system

Tianhe Yu (于天河)[1,2*], Qiuming Li (李秋明)[3], and Jingmin Dai (戴景民)[1]

[1]*Department of Automation Measurement and Control Engineering, Harbin Institute of Technology, Harbin 150001*

[2]*Computer Center, Harbin University of Science and Technology, Harbin 150080*

[3]*School of Astronautics, Harbin Institute of Technology, Harbin 150001*

[*]*E-mail: ythaa@163.com*

Received September 18, 2008

Infrared images are firstly analyzed using the multifractal theory so that the singularity of each pixel can be extracted from the images. The multifractal spectrum is then estimated, which can reflect overall characteristic of an infrared image. Thus the edge and texture of an infrared image can be accurately extracted based on the singularity of each pixel and the multifractal spectrum. Finally the edge pixels are classified and enhanced in accordance with the sensitivity of human visual system to the edge profile of an infrared image. The experimental results obtained by this approach are compared with those obtained by other methods. It is found that the proposed approach can be used to highlight the edge area of an infrared image to make an infrared image more suitable for observation by human eyes.

OCIS code: 100.0100.

doi: 10.3788/COL20090703.0206.

Histogram equalization is an algorithm most commonly used to enhance infrared images. This algorithm can effectively enhance the contrast of an infrared image. However, it also causes an excessive enhancement of details and the occasional loss of edge details and features, which undoubtedly have an adverse effect on the visual effects of infrared images. The information contents are different in different areas of an image, and so is their importance. In reality, it is not the whole image that contains the same important information for an observer, and it is more often that the observer is interested in part of the image only. It is usually human eyes that evaluate the final results of image enhancement, and so a very good visual effect can be obtained if enhancement of infrared images is based on a human visual system (HVS).

Most of the image enhancements used at present are in the space or frequency domain and few are fractal based ways. According to the fractal theory, fractal is a more common and typical phenomenon over a natural surface. Like many natural images, infrared images have much randomness in structure and noise. The gray scale of an image is a coarse surface suitable for the description and analysis of fractal when it is taken as the height of a plane. Xia *et al.* have successfully applied fractal to geographic simulation, grain analysis, segmentation, and identification of images[1,2]. In this letter, we present the application of fractal in the field of image enhancement. The dimensions of fractal represent the similarity of images, not the gray scale, but the relationship between one point and the surrounding points. When the fractal dimension is used to enhance an image, the different gray segments in the time domain and several frequency ranges in the frequency domain are considered.

A variety of visual masking effects have been discovered through physiologic and psychologic researches on the vision of human eyes[3,4]. As shown in Fig. 1, the analysis of contrast sensitivity function indicates that human eyes are much more sensitive to the changes in the low frequency area than those in the high frequency area. From the viewpoint of space frequency, human eyes are a low-pass linear system with limited scene distinguishing capacity and HVS is not sensitive to an excessively high frequency. The perceptual experiments on the perception of human eyes indicated that the attention of human eyes is always concentrated on the fragmentation and characteristic profile of the object with all the ordinary details totally neglected when human eyes are sensing a natural object. In Fig. 1, $H(w)$, which is a normalized parameter, is the sensitivity function of vision frequency response.

It is known through psychologic researches that an image consists of three components with different perceptual significances: smooth area, edge area, and texture area. An area is called a smooth area if the change in its gray scale is gentle, and an area is called an edge area if the change in its gray scale is severe. The density of edges in an edge area is the basis for differentiation of an edge area from a veined area. Images with different information contents can thus be simply classified according to HVS.

It can therefore be concluded that human eyes are

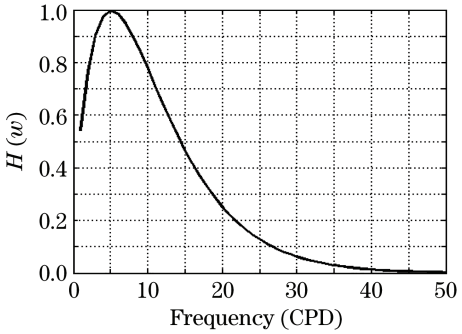

Fig. 1. Function of vision frequency response.

very sensitive to the distortion of information in the edge area of an image, more sensitive to the one in the smooth area, and not sensitive to the one in the veined area. The sensitivity of human eyes varies with the edge area, smooth area, and texture area of an image, which means there is a difference in the importance of information in the texture area of an image. Therefore, the information to which human eyes are sensitive can be enhanced maximally by weighting the fractal dimension corresponding to the information contained in the three different areas.

The multifractal dimensions represent the similarities of images. It does not accord to the gray scale of the pixels themselves, but accords to the relationship of one point and the surrounding points[5−7]. The fractal dimensions at this point can be obtained from the change in the gray scale of one of its neighboring points. The characteristics of an image signal cannot be fully described by a single fractal dimension. It is known through experiments that many images with a very big difference in visual effects have a very similar fractal dimension. In order to describe an image with more details, more parameters are needed for the description of different fractal subsets. This is the reason why multifractal theory is introduced.

When multifractal analysis is used, not only the geometrical features but also the statistical feature of the edge at different dimensions are taken into consideration by using Hölder exponent α and multifractal singularity spectrum $f(\alpha)$, respectively, so that the detailed information at the main edges can be highlighted while the unimportant edges are neglected. The drawback of doing so is its higher sensitivity to noise. But it can be remedied by defining the following parameters when supposing Ω is the area of an image:

$$\mu_{\max}(\Omega) = \max(I(x,y)), \tag{1}$$

$$\mu_{\min}(\Omega) = \min(I(x,y)), \tag{2}$$

$$\mu_{\text{sum}}(\Omega) = \text{sum}(I(x,y)), \tag{3}$$

$$\mu_{\text{iso}}(\Omega) = \text{iso}(I(x,y)), \tag{4}$$

where $(x,y) \in \Omega$, $\mu_{\max}(\Omega)$ is the maximum gray scale of a pixel in the area Ω, $\mu_{\min}(\Omega)$ is the minimum gray scale of a pixel in Ω, $\mu_{\text{sum}}(\Omega)$ is the sum of some pixels in the area, $\mu_{\text{iso}}(\Omega)$ is the importance of the maximum subsets with the same gray scale in the area. If there are N pixels of different gray scales in an area, $\mu_{\text{iso}}(\Omega) = 1$. If all the pixels in an area have the same gray scale, $\mu_{\text{iso}}(\Omega) = N$. The singularity of these measurements represents different information. $\mu_{\max}(\Omega)$ and $\mu_{\min}(\Omega)$ relate to the height of singularity only, $\mu_{\text{sum}}(\Omega)$ relates to both height and type of singularity, and $\mu_{\text{iso}}(\Omega)$ relates to the type of singularity only. Each measure has its own parameters, and different images have different statistical features. So, it is necessary during the calculation to decide through experiments and error analyses what measures should be used to achieve the best visual effect.

We have a Hölder exponent α_n at position

$$I_{i,j,n} \cdot \alpha_n(I_{i,j,n}) = \frac{\log \mu(I_{i,j,n})}{\log V_n}. \tag{5}$$

Supposing μ is the probability measure over $[0,1] \times [0,1]$, and V_n is an incremental series consisting of positive integers, then

$$I_{i,j,n} = \left[\frac{i}{V_n}, \frac{i+1}{V_n}\right] \times \left[\frac{j}{V_n}, \frac{j+1}{V_n}\right]. \tag{6}$$

Considering

$$\tau_n(q) = \frac{i}{\log V_n} \log \sum_i{}^* \sum_j{}^* \mu(I_{i,j,n})^q, \tag{7}$$

where $\sum_i{}^*$ is the sum of $\mu(I_{i,j,n}) \neq 0$ pixels. When there is a limit, it is supposed that

$$\tau(q) = \lim_{n \to 0} \tau_n(q). \tag{8}$$

The Legendre transformation from $\tau(q)$ to $f_l(\alpha)$ is defined as

$$f_l(\alpha) = \inf_{q \in R}(q\alpha(q) - \tau(q)). \tag{9}$$

The calculation of multifractal parameters entails a much larger amount of computational work[8,9], so some computational techniques or approximation methods are usually used. For a nonuniform measurability distribution, $f(\alpha)$ is a unimodal convex function of α. For a uniform measurability distribution, the modal curve is compressed into a beeline. According to multifractal theory, $f(\alpha)$ is called the singular spectrum of multifractal. A fractal set can be quantitatively described by $f(\alpha)$. Multifractal analysis is very effective in processing signals of singular structure. Local information can be obtained from the Hölder exponent of α at each point while global information can be obtained from the multifractal singularity spectrum of the whole image.

The following is the image edge detection algorithm used for multifractal frequency analysis.

Step 1: Select the α capacity series and the reference measurability μ, so that the area Ω is a pixel area of 3×3.,

$$\alpha(x,y) = \lim_{k \to 0} \frac{\ln(\mu(V(k))}{\ln(k)}. \tag{10}$$

Step 2: Supposing Q is an image area, $I(x,y)$ represents the gray scale of point (x,y), the singularity exponent α represents the local singularity of an image. $V(k)$ is defined as a square neighboring area of $k \times k$ pixels, and the central point is the interesting point expressed by $I(x,y)$. $\alpha(x,y)$ can be estimated from the slope of $\ln(\mu(V(k))$ and $\ln(k)$. k relates to the arithmetic location. If a small neighboring area is used, for example, $k \leq 3$, $\alpha(x,y)$ reflects the local singularity. If a big neighboring area is used, α reflects a wider singularity. As shown in Fig. 2, the image is formed by the singularity indices of infrared images.

Step 3: There is a great variety of α obtained by calculating the singularity exponent as specified in step 1. The following can be obtained by calculating the maximum and minimum of the singularity exponent for each point (x,y): $\alpha_{\max} = \max(\alpha(x,y))$, $\alpha_{\min} = \min(\alpha(x,y))$. $[\alpha_{\max}, \alpha_{\min}]$ is subdivided into N boxes and $N(\alpha)$ to which α belongs is counted.

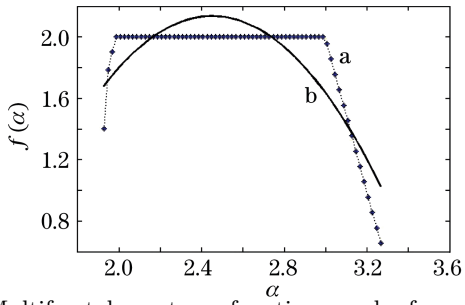

Fig. 2. Multifractal spectrum function graph of an actual infrared image.

Step 4: $f(\alpha)$ represents the global singularity of an image, and for singularity exponent α of each point (x, y), $f(\alpha)$ can be obtained using the following equation usually through the linear regression of $(\log N(\alpha), \log n)$,

$$f(\alpha) = \lim_{n\to\infty} \frac{\log N(\alpha)}{\log n}. \tag{11}$$

Multifractal spectrum, a two-dimensional (2D) parabola, can be obtained by α and $f(\alpha)$ as shown in Fig. 2. The multifractal nature of the infrared image can be seen from the shape of the 2D parabola obtained by fitting the actual infrared image. In Fig. 2, the curve a is plotted by data α and $f(\alpha)$, and the curve b is obtained by fitting all points of curve a.

Step 5: Classify the pixel points of an image according to the multifractal frequency spectrum. The multifractal frequency spectrum of ordinary edge pixel points remains in the range of $\alpha \le 1.2$, $1.0 \le f(\alpha) \le 1.5$. The greater the threshold is, the finer the detected edge is.

The boundary point of an infrared image is the point to which human eyes are sensitive. Better visual effects can be obtained by enhancing these pixels. So the gray scale of the pixels in the boundary area must be stretched so that a brighter or darker sense can be generated, which differentiates it from the pixels of non-boundary points, thereby solving the problem of blurred edge of infrared images. As human eyes are not sensitive to the noise in the high frequency area of the boundary, the enhancement of these pixel points will not result in the excessive enhancement of noise.

According to the size of the sub-dimensional singular feature of each point, each pixel is classified as detailed, smooth, and veined. What has been obtained in the previous steps is a matrix used to characterize the singularity α of each pixel and a mapping with $\alpha \to f(\alpha)$, where $f(\alpha)$ is used to characterize the frequency at which α appears. According to its way of calculation, a rule has been defined as follows: the point corresponding to this α is the uniform texture of an image when $\alpha \le 1.2$ and $1.5 \le f(\alpha) \le 1.8$; the pixel point corresponding to α is the boundary in an image when $\alpha \le 1.2$ and $1.0 \le f(\alpha) \le 1.5$; the pixel corresponding to α is in the smooth area of an image when $1.8 \le f(\alpha) \le 2.0$.

The edge of an image is enhanced using a bigger weight. A weight of 1.2 is used for a smooth area; a weight of 1.4 is used for a veined area; and a weight of 1.6 is used for a boundary area. The pixels in the boundary area of an infrared image must be enhanced so that stronger contrast can be generated to solve the problem of blurred edge of an infrared image.

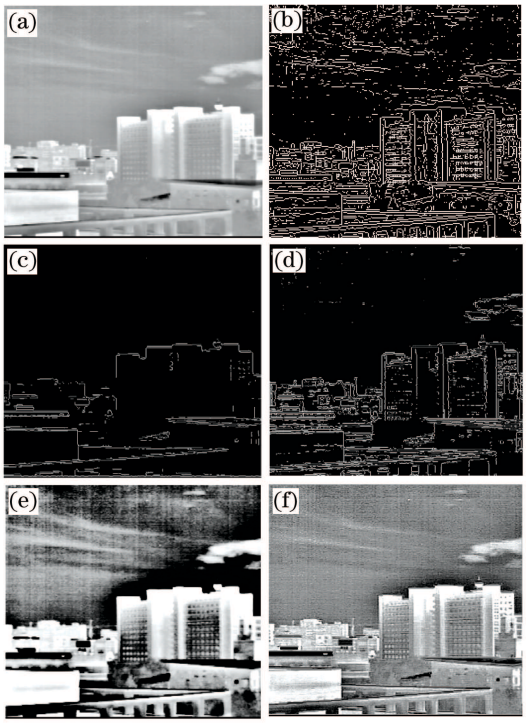

Fig. 3. Comparison of enhancement effect. (a) Original image; (b) edge image by Soble algorithm; (c) edge image with $1.0 < f(\alpha) < 1.1$; (d) edge image with $1.0 < f(\alpha) < 1.3$; (e) after histogram equalization; (f) by the proposed method.

Infrared images of 256×256 pixels are used to evaluate the effectiveness of the algorithm proposed in this letter. In order to better reflect the characteristics of height type of an image, the multifractal singularity is measured using the sum of pixel areas. The enhancement results are shown in Fig. 3. Figure 3(a) is an original image not suitable for observation by human eye for the darker image without strong contrast, and it has a blurred edge and the gray scale is distributed at a lower level. In Fig. 3(b), the edge is extracted using the Sobel algorithm. In Figs. 3(c) and (d), the edge is extracted using the proposed algorithm. It can be seen that the edge is fully extracted and HVS is sensitive to these edges.

As shown in Fig. 3(e), the contrast has been enhanced through histogram equalization, but some details are so excessively enhanced that they are illegible. While in Fig. 3(f), the details of buildings and trees are detected with the brightness improved. And the highlighted detailed features are just in conformity with HVS. With a proper $f(\alpha)$ selected, the edge detection method based on multifractal frequency analysis can be used to detect the linear edge of an image, and local highlight can be achieved by enhancing the pixel in this area.

In order to detect and enhance the edge of an infrared image, the Hölder exponent $\alpha(x, y)$ of a pixel point is calculated, and its multifractal frequency spectrum $f(\alpha)$ is then estimated. The distributions of the multifractal spectrum of pixels reflect the structure of an image. The edge of an image detected by a singularity measure is an accurate local edge. The accuracy of edge detection can be controlled by adjusting the range of $f(\alpha)$ in accordance with the size of an edge required. The pixels of an infrared image are then classified by their edges in accor-

dance with the sensitivities of human eyes. Each pixel is enhanced by weighting. It has been proved through comparative experiment with histogram equalization that the method proposed here can be used to directly enhance the details in which human eyes are interested so that the enhanced image has a better visual effect, thereby solving the problem of blurred infrared image.

This work was supported by the Natural Science Foundation of Heilongjiang Province under Grant No. F200818.

References

1. G. Xia and B. Zhao, Chin. Opt. Lett. **5,** 51 (2007).
2. G. Wang, L. Xiao, Z. Jiang, Y. Song, and A. He, Acta Opt. Sin. (in Chinese) **26,** 1345 (2006).
3. T.-L. Ji, M. K. Sundareshan, and H. Roehrig, IEEE Trans. Med. Imaging **13,** 573 (1994).
4. K. A. Panetta, E. J. Wharton, and S. S. Agaian, IEEE Trans. Syst. Man Cybern. B **38,** 174 (2008).
5. J. Zhao, C. Yang, and B. Yu, Acta Photon. Sin. (in Chinese) **32,** 61 (2003).
6. K. Ferens and W. Kinsner, in *IEEE WESCANEX '95 Proceedings* 438 (1995).
7. I. Reljin, B. Reljin, I. Pavlović, and I. Rakočević, in *Proceedings of 10th Mediterranean Electrotechnical Conference* **2,** 490 (2000).
8. J. Liu, K. Bowyer, D. Goldgof, and S. Sarkar, in *Proceedings of 1997 International Conference on Information, Communications and Signal Processing* 170 (1997).
9. B. B. Chaudhuri and N. Sarkar, IEEE Trans. Pattern Anal. Mach. Intell. **17,** 72 (1995).